Available online at www.sciencedirect.com

ScienceDirect

Transportation Research Procedia 2 (2014) 77 – 86

Transportation Research Procedia

www.elsevier.com/locate/procedia

The Conference on Pedestrian and Evacuation Dynamics 2014 (PED2014)

Density and velocity patterns during one year of pedestrian tracking

Dražen Brščić [a,b], Francesco Zanlungo [a,b,*], Takayuki Kanda [a,b]

[a] *IRC-ATR, Kyoto, Japan*
[b] *JST CREST Tokyo, Japan*

Abstract

We tracked the movement of people during a one year span in a shopping mall to study pedestrian behaviour under different density and usage conditions. We analyse the time and space dependence of pedestrian density and velocity, showing good agreement with the predictions of our "social norm" collision model. We also show that along with the expected decrease of velocity with growing density, we find density independent time patterns, corresponding to higher velocity in working days and during "rush hours", and also a general tendency to have slower velocities in later hours. We also report a positive correlation of pedestrian velocity with human height, an effect weaker on weekends

Peer-review under responsibility of Department of Transport & Planning Faculty of Civil Engineering and Geosciences Delft University of Technology

Keywords: flow splitting; density velocity relations

1. Introduction

Models of crowd behaviour may be roughly divided between those that use a macroscopic approach, i.e. that are interested only in describing macroscopic crowd observables, such as density and flux Kachroo et al. (2008), and those that use a microscopic approach, i.e. that provide a model for the behaviour of individual pedestrians; the second approach, either in its continuous Helbing and Molnar (1995); Guy et al. (2012); Zanlungo et al. (2011) or discrete Burstedde et al. (2001); Muramatsu and Nagatani (2000) form, is probably mainstream in current studies. Nevertheless, the knowledge of the macroscopic behaviour of crowds is essential even when the description of the dynamical law is performed at a strictly microscopic level, since after all one of the purposes of all pedestrian models is to reproduce the overall crowd dynamics, and in order to test and calibrate any kind of model, a comparison with the behaviour of real crowds in some benchmark situation is necessary.

Between the most commonly used benchmark situations there is the behaviour of pedestrians in a corridor in the case of a single and double flow Helbing et al. (2002). The former case *appears* to be of a striking conceptual simplicity, since we may expect to describe the behaviour of the crowd in such a situation through a single function relating the average velocity of the crowd to the density, while in the second case we expect to have to describe also the sepa-

* Corresponding author. Tel.: +000-000-000-000; fax: +000-000-000-000
E-mail address: zanlungo@atr.jp

Peer-review under responsibility of Department of Transport & Planning Faculty of Civil Engineering and Geosciences Delft University of Technology
doi:10.1016/j.trpro.2014.09.011

ration of the flows[1]. The single flow case velocity-density dependence goes under the name of "fundamental diagram" of pedestrian dynamics Seyfried et al. (2005). It is nevertheless not very surprising that, despite the "fundamental" nature of the problem, very little consensus is present about the behaviour of crowds in such a situation, due to the difficulty of collecting quantitative data about the behaviour of pedestrians in real world environments. The recent development of sensors and corresponding algorithms for automatic pedestrian tracking (see e.g. Bauer et al. (2009)) is arguably going to change the situation in the coming years. In this paper we are going to show the results of a one year long campaign of automatic tracking of pedestrians in a real world environment. By analysing the density and velocity pedestrian patterns in a corridor located in this environment, we hope to provide a new insight on these fundamental problems in pedestrian studies.

2. Environment, person tracking and collected data

The Asia and Pacific Trade Center, located in the Osaka Port area, is a large multi-purpose centre, that includes exposition halls, shops, offices, restaurants, sport facilities, a ferry terminal and a train station, with a total floor space of 336000 m^2. The data collection was done in a 900 m^2 area of the second floor, consisting mainly of a large square, where small events are often held, and a relatively narrow corridor. This corridor is one of the main connecting ways of the building, being situated between the area where the offices and ferry terminal are located and the area where most restaurants and shops are situated. It also represents the access to the train station from the office area.

To track the persons inside the area we installed 3D range sensors on the ceiling, in total 49 of them. This type of sensors has an advantage over standard cameras in that it is less influenced by lighting conditions so robust tracking during long periods of time is possible. Combining all sensors allows us to obtain data on the position, height and body orientation of all the pedestrians in the area. The complete details about the tracking method and the obtained tracking performance are given in Brščić et al. (2013).

We automatically tracked the movement of pedestrians in the environment for 84 days (43 Wednesdays and 41 Sundays from October 24, 2012 to September 29, 2013), 10 hours and 40 minutes a day (from 9:40 to 20:20)[2]. The average density of *moving* pedestrians (defined as pedestrians with velocity $v > 0.5$ m/s) in the tracked environment during non-working days is shown in Fig. 1a. On the right side of the tracked environment we have the corridor, in which, despite the absence of straight delimiting walls (due to the presence of stand areas on the sides, Fig. 1b[3]), we have a very well delimited flow of pedestrians (high density moving pedestrian area, shown in blue in Fig. 1a.) For the purpose of this paper we will focus only on the analysis of data from a straight area of the corridor, shown in the black box of Fig. 1a. Fig. 1c shows, for each 0.25 m^2 cell in the studied portion of the environment, the average velocity vector, highlighting the splitting of the two flows, with pedestrians walking prevalently on the left side, as it is usual in Japan Zanlungo et al. (2012).

3. Flow splitting

3.1. Statement of the problem

We restrict our attention the portion of the corridor highlighted in Fig. 1. According to Helbing et al. (2002), we expect a separation of the flow of pedestrians depending on their direction. Such a separation minimises the possibility of collisions and maximises the pedestrian flux, and it is predicted by most microscopic pedestrian models Zanlungo (2007). Nevertheless, a completely symmetrical model cannot describe the fact that the separation happens in prevalence on a given side of the corridor (the particular side being culture dependent, corresponding to the left side in Japan, as shown in Fig. 1). Such a result can be attained by introducing a bias in collision avoiding Moussaïd et al. (2009). In Zanlungo et al. (2012) we introduced two different ways of describing such a bias, one based on relative

[1] Obviously in both cases we shouldn't expect the density and velocity patterns to be uniform in the whole corridor, as we show in Zanlungo et al. (2012) and in the present work for the counterflow case.

[2] A sample of the tracking dataset is freely available from `http://www.irc.atr.jp/crest2010_HRI/ATC_dataset/`

[3] This stands are movable, and actually their configuration changed considerably during the year. Nevertheless, they are located outside the investigated area, and represent its "boundary conditions". The fact that the (walking) pedestrian density goes to zero at the boundaries (Fig. 2) suggests that this effect on the dynamics should be negligible.

(a) (b) (c)

Fig. 1: (a): density of pedestrians walking with a velocity $v > 0.5$ m/s, in the whole environment, averaged over all non-working days. Red corresponds to low density, blue to high density, white to absence of data. The black box shows the "corridor area" whose density and velocity profiles are analysed in this paper. (b): pictures of the corridor area. (c): average velocity vector in each 0.25 m^2 cell in the corridor area (black box in Fig. 1a). Red arrows show velocities whose main component is directed towards up-left, blue ones velocities whose main component is directed towards down-right. The splitting of the flows, with pedestrians walking on the left side of the corridor, is evident.

position, and the other one based on the relative velocity. We suggested that the second method (velocity bias) better reproduces pedestrian behaviour, since it may be described through a simple behavioural rule (this rule may be stated as "expecting that everybody will avoid collision preferentially on the left and acting in consequence (by changing one's velocity)"). We also showed that while the two models describe (qualitatively) the same density distribution patterns (pedestrian walking on the left side of the corridor), their velocity distributions are very different, with the first method (position bias) predicting pedestrians with higher velocity to walk close to walls, while the second method predicts faster pedestrians to walk in the centre of the corridor. Our observations confirmed that the second method correctly describes (Japanese) pedestrian behaviour.

In order to properly calibrate a microscopic model on the splitting of opposite flows in a corridor it is, nevertheless, necessary to know how this splitting changes over a significant range of pedestrian densities. As we showed in Zanlungo et al. (2014), at fixed density it is possible to describe the flow splitting as due to a tendency of pedestrians to walk on the left, *regardless* of collision avoidance, or even as the combination of a collision independent and a collision dependent term. Leaving a quantitative analysis (both from a simulation and a theoretical point of view) for a future work, we may expect that if the flow splitting is due exclusively to collision avoidance, it should increase with the pedestrian density and disappear in the $\rho \to 0$ limit. By analysing more than 800 hours of data, in this paper we try to answer to this question.

3.2. Data analysis

We analysed the pedestrian data in an area of length 12 meters and width 3.5 meters[4], excluding all data points k with velocity $v_k < 0.5$ m/s and considered only trajectories whose time length *in the whole tracking environment* was $T > 10$ s and that had an average (vectorial) velocity of at least $\overline{v} = 0.5$ m/s (i.e. the displacement was more than $T\overline{v} = 5$ m). These filtering choices have two reasons: removing any source of noise and focusing only on moving pedestrians. We then divided our data in time slots of 20 minutes, and for each time slot we computed the average pedestrian density[5]. For each data point k we computed $v_k^x \equiv \mathbf{v}_k \cdot \mathbf{i}$, where $\mathbf{i}$ is the unit vector of the axis of the corridor, and divided the pedestrians in two groups, depending on their walking velocity, as $P^{\mathrm{pos}} = \{k | v_k^x > 0\}$, $P^{\mathrm{neg}} = \{k | v_k^x < 0\}$. Depending on the moment of the day, one of the two flows may be much stronger than the other, but in order to reduce the parameters on which the separation of flows may depend, in the following analysis we will consider only time slots in which to none of the two direction flows corresponded more than 60% of the overall pedestrian density[6].

[4] We choose this area since it presented an almost straight flux, invariant along its main axis direction. Since the corridor does not have well defined walls, its width has been determined considering the borders at which the moving pedestrian density became negligible.

[5] As $\sum_j N_j/(A \sum_j j)$, where j is the set of all tracking instants in the time slot, N_j the number of pedestrians tracked at time j and A the size of the area.

[6] This condition is satisfied in 56% of the time slots. In this analysis we ignore any other dependence of the separation of flows on variables different from the overall density. This is necessarily an oversimplification, since we may expect, based on simple considerations on the collision

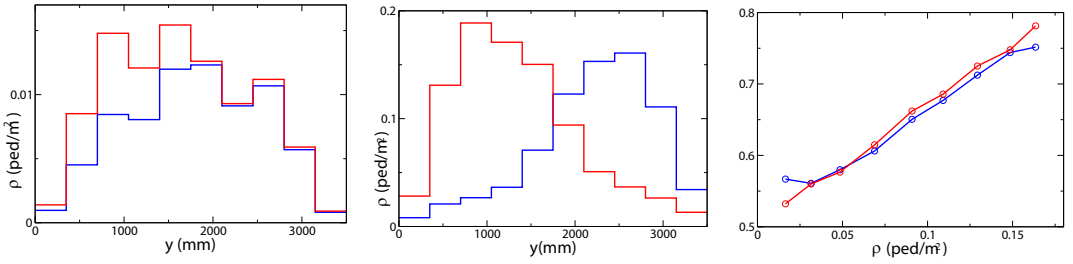

(a) (b) (c)

Fig. 2: (a): $\rho_m^{(0,+)}$ (red) and $\rho_{9-m}^{(0,-)}$ (blue), i.e. a comparison of the separation between the two flows at a density $0 \leq \rho < 0.02$ ped/m^2. (b): $\rho_m^{(8,+)}$ (red) and $\rho_{9-m}^{(8,-)}$ (blue), i.e. same comparison for $0.16 \leq \rho < 0.18$ ped/m^2. (c): ρ_l as a function of the pedestrian density; strongest flow in red, weakest in blue.

For each 20 minutes slot we compute the average density $\rho_m^{\text{pos,neg}}$ and average velocity $v_m^{\text{pos,neg}}$ in 10 "microlanes" of width $\Delta y = 0.35$ m, for each flow direction. The numbering $m = 0, ..., 9$ starts, for each flow, from the left "wall" (left as seen by the walking pedestrians), i.e. the lane with $m = 0$ is the closest to the left wall, while the one with $m = 9$ is the closest to the right wall. After computing these variables, we rename ρ_m^+ and v_m^+ as the density and velocity in the flow with higher density, and ρ_m^- and v_m^- as the density and velocity in the flow with lower density (in order to give always the same role to the slightly stronger flow). Finally, we divide the time slots depending on their overall average density (i.e. as averaged on all lanes and summed over the two flows), and average the resulting distributions over all slots falling in the $[n\Delta\rho, (n+1)\Delta\rho)$ density range, with $n = 0, ..., 8$, $\Delta\rho = 0.02$ ped/m^2. We will thus name $\rho_m^{(n,+)}$ the average density in the stronger flow, at a distance $m\Delta y \leq y < (m+1)\Delta y$, averaged on all data with overall environment density between $n\Delta\rho$ and $(n+1)\Delta\rho$. Equivalent definitions are given for $\rho_m^{(n,-)}$ (weaker flow) and for average velocities $v_m^{(n,\pm)}$ (here and afterwards we use $\pm$ as shorthand for values in both stronger and weaker flows).

Fig. 2 compares the (a) $\rho_m^{(0,\pm)}$ and (b) $\rho_m^{(8,\pm)}$ distributions (for easier visualisation of the flow separation we have plotted $\rho_{9-m}^{(-)}$, i.e. for the minor flow *the left wall is on the right*). It is clear that with higher density the flows are more separated. Let us measure quantitatively the effect of density, by defining, for each flow, the relative density of pedestrians on the left side of the corridor, as:

$$\rho_l^{(k,\pm)} = \frac{\sum_{m=0,...,4} \rho_i^{(k,\pm)}}{\rho_{\text{tot}}^{(k,\pm)}}, \qquad \rho_{\text{tot}}^{(k,\pm)} = \sum_{m=0,...,9} \rho_i^{(k,\pm)}. \tag{1}$$

It is clear that we should have $\rho_l = 1$ in case of complete separation, and $\rho_l = 0.5$ if no separation occurs. The dependence of ρ_l on density is shown in Fig. 2c. The results seem in agreement with the hypothesis that the flow splitting is absent in the low density limit ($\lim_{\rho\to 0} \rho_l = 0.5$). ρ_l seems to grow linearly with ρ in the investigated range[7]. Provided that future works should investigate also the dependence of these results on the corridor's width, our findings support the idea that the splitting of flows is due to the microscopic interaction (collision avoidance)[8], and provide an empirical function on which microscopic models may be tested.

avoidance behaviour, that also the average velocity and number of groups (which, as we show in the next section, vary strongly depending on the moment of the day and between working days and non-working days) may influence the flow separation. In this work we show the main effect of the density variable, and leave for future work the analysis of the dependence on other factors.

[7] Clearly since we have by definition $\rho_l < 1$ we should have a saturation value for the growth of the split, but this value appears to be beyond the maximum density found in our environment.

[8] Obviously, pedestrians may still use a collision independent mechanism, such as walking preferentially on the left *depending on the overall pedestrian density*. In such a situation, a model like the one we proposed in Zanlungo et al. (2014) could be used to describe the process, establishing a connection between the inverse temperature β and the overall density. Furthermore, a tendency to walk on the left even at very low densities could be present in a larger corridor, or even in a narrow environment with better defined walls.

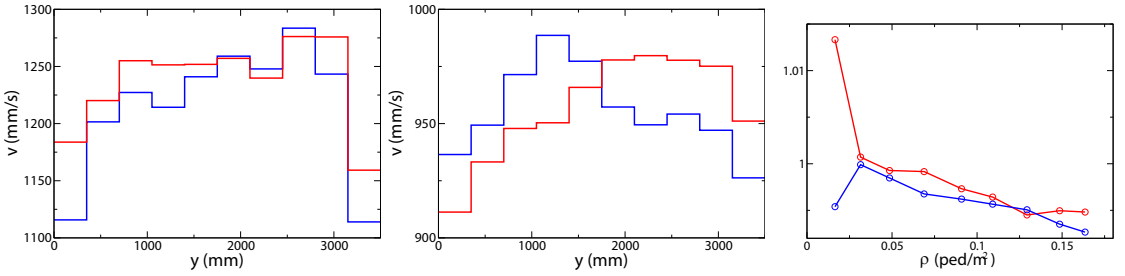

(a) (b) (c)

Fig. 3: (a): $v_m^{(0,+)}$ (red) and $v_{9-m}^{(0,-)}$ (blue), i.e. comparison of the velocity profiles in the two flows as a function of the distance from the left wall y at density $0 \le \rho < 0.02$ ped/m^2. (b): $\rho_m^{(8,+)}$ (red) and $\rho_{9-m}^{(8,-)}$ (blue), i.e. same comparison for $0.16 \le \rho < 0.18$ ped/m^2. (c): v_l as a function of the pedestrian density; strongest flow in red, weakest in blue.

Figs. 3a and 3b compare the $v_i^{(0,\pm)}$ and $v_i^{(8,\pm)}$ distributions, respectively. Even though the effect is obviously not so clear as for the density, it seems that a transfer of higher velocities to the right with growing densities is present. Let us measure quantitatively the effect of density, by defining the ratio between the average velocity on the left with respect to the overall average velocity:

$$v_l^{(k,\pm)} = \frac{\sum_{m=0,\dots,4} v_m^{(k,\pm)} \rho_m^{(k,\pm)}}{\left(\sum_{m=0,\dots,9} v_m^{(k,\pm)} \rho_m^{(k,\pm)} \right) \rho_l^{(k,\pm)}}. \tag{2}$$

The dependence of v_l on density is shown in Fig. 3c. We may say that there is a tendency, at higher densities, to have higher velocities for pedestrians walking far from the left wall, confirming the results of Zanlungo et al. (2012). Once again, these findings may be used to test microscopic pedestrian models (in particular in their description of overtaking behaviour).

4. Variables determining pedestrian velocity

Strictly speaking, we cannot use the data from the corridor to study the "fundamental diagram" problem, due to the presence of two opposite flows. Nevertheless, we may try to study all the factors that affect the pedestrian velocity in our environment, including the density independent ones, to try to shed light on the reasons that always made the study of velocity-density relations particularly difficult.

We restrict again our attention to the corridor and to pedestrians that move fast enough and are being tracked in a stable way (by applying the same filtering of section 3). As it will be clear in the discussion below, the velocity patterns during working days and non-working days are quite different, and for this reason we will split our data analysis between Wednesdays and Sundays. We will consider nevertheless 3 Wednesdays as non-working days[9]. We have thus 40 days that are classified as working days, and 44 classified as non-working days.

[9] March 20th 2013 (a national holiday in Japan), May 1st 2013 and August 14th 2013. While these latter days were not national holidays, they fall (respectively) in the "Golden Week" and "O-Bon" periods, which are, along with the days around New Year (in which we didn't collect data) the periods of the year in which many Japanese take holidays.

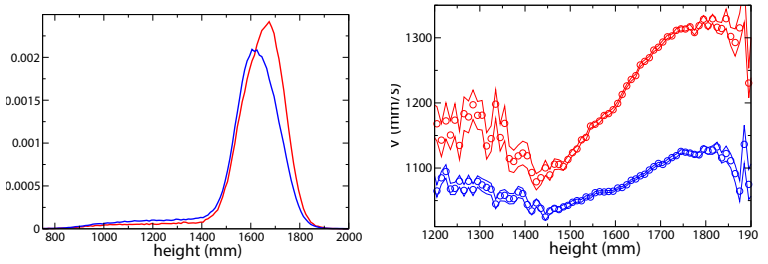

(a) (b)

Fig. 4: (a): pdf for pedestrian height, in working days (red) and non-working days (blue). (b): pedestrian velocity as a function of height; working days in red and non-working days in blue. Circles represent point data, while continuous lines represent standard error ranges.

4.1. Height and velocity

We first study how the velocity depends on the pedestrians' stature. Fig. 4a shows the probability density function for the pedestrian height[10], which results to be significantly different between working days and non-working days, due probably to an higher relative number of adult workers during working days. The maximum of the distribution falls between 1.6 and 1.7 meters, in agreement with the values for the average height of adult Japanese[11]. For each pedestrian we then measure the average height and velocity, and plot the results (averaging in 1 cm slots) in Fig. 4b. We find an almost linear growth between 1.45 and 1.8 meters (i.e. corresponding to the main component of the height distribution), even though the growth is weaker during non-working days[13].

4.2. Time variation of density

Since we expect the pedestrian velocity to change with the density in the environment, let us evaluate the time variation of the density. Furthermore, considering the influence of height on velocity, we will also evaluate the density of people with height between 160 and 190 cm ("tall people", including probably a large number of adults) and below 160 cm ("short people", including probably a large number of children).

Fig. 5 shows the hour dependence of the density of people in (a) working days and (b) non-working days. We may see that the daily density time pattern for "tall" and "short" people is similar in non-working days, attaining a plateau between 12 and 18. The pattern for "short" is similar in working days, but for "tall" we have strong maxima at 12 and 18. These maxima correspond to the moment at which workers go to lunch and come back, and to when they leave work[14].

4.3. Time variation of velocity

Fig. 6 shows the time dependence of velocity during the day[15]. Three different values are shown, corresponding to the overall distribution, and to "tall" and "short" people.

---

[10] For each trajectory we compute the average height, then the probability is computed over height intervals of 1 cm.

[11] In the year 2013 the average height of 17 year old high school students was 170.6 cm for males and 157.8 cm for females [12].

[13] The effect is less clear when the whole height range is observed. This is probably due not only to the small samples, but also to some incorrect tracking of objects (carts, etc.) as people.

[14] If we analyse the peaks in the two directional flows, we find two peaks in the flow directed to the restaurants and station, at 12 and 18, and a single peak towards the offices, just before 13.

[15] The velocities shown correspond to the centre of the Gaussian distribution that better fits the observed velocity distributions. The best fitting Gaussian is obtained for each 20 minutes slot, and the results are averaged over the whole year, computing standard errors based on the yearly variation at a given time of the day.

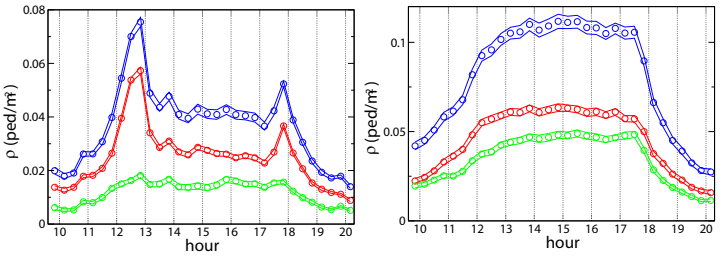

Fig. 5: (a): time variation of density as a function of day time in working days. Overall density in blue, "tall people" in red, "short people" in green; (b): same graph for non-working days.

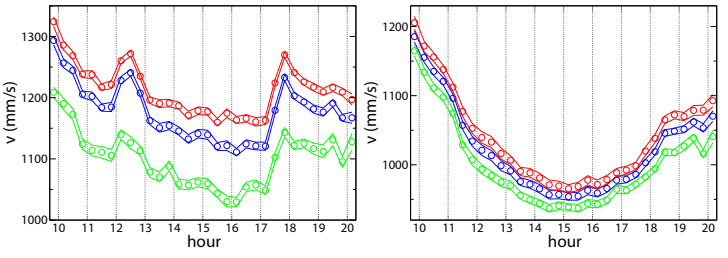

Fig. 6: (a) Dependence of pedestrian velocity (centre of best fit Gaussian) on the hour of a working day. Overall distribution in blue, "tall people" in red, "short people" in green. (b): same graph for non-working days.

Comparing to Fig. 5 we see that in general, as expected, velocities are slower when the density is higher. Nevertheless, a more complex time dependence is present. First of all, velocities are in general slower on non-working days, even at low densities. Furthermore, the working day velocity distribution attains local maxima at 12 and 18, i.e. when also density attains maxima. The different behaviour shown at these times ("rush hours") makes the pedestrians walk faster even if the density is higher; most probably the nature of the pedestrians is also different (these maxima are attained when the relative number of "short people" is lowest). It seems also that there is a tendency for velocities to be lower in the later hours on the day, a tendency that is particularly clear on non-working days. We also notice that the difference in velocity between "tall" and "short" people is reduced in non-working days. These results seem to suggest that "tall people" are slower when a higher *relative number* of "short people" are around. This is probably due to two effects, the presence of mixed groups of children and adults, walking at similar velocities, and the fact that when more children are around, probably also a larger number of adults in the environment are "leisure oriented"[16]. These results may also explain why the height dependence of velocity is weaker on non-working days.

[16] It may also be that, at higher densities and with a relatively higher number of short people, the motion of tall ones is more hindered. But this hypothesis seems in contrast with the finding that the difference in "tall" and "short" velocities is reduced even when the density is very low in non-working days, see figures 5 and 6.

4.4. Density dependence of velocity

Fig. 7a shows a velocity versus density graph for all 20 minutes time slots and compares it to a linear model,

$$v(\rho) = v_{\rho_0} + b_\rho \rho, \tag{3}$$

which appears to be adequate for non-working days (after an initial flat area) but fails to describe the working day behaviour at high density (due to the "rush hours" behaviour at 12 and 18). Obviously, in both cases the variation is large around the linear behaviour. Even if assuming a linear dependence on density is just a rough approximation, we may use the linear model of Fig. 7a (and similar models obtained for "tall" and "short" people velocity, see Table 1) to extrapolate the "zero density velocity" (the theoretical value of the velocity if the density were equal to zero) from the data of Fig. 6, as

$$v_{\rho_0}(t) = v(t) - b_\rho \rho, \tag{4}$$

where t is the time of the day. The time dependence of these velocities is shown in Fig. 8. The most significant insight of these graphs is probably related to the clear decrease of velocities with growing time during the day on non-working days; such a pattern is present also on working days but is contrasted by the presence of the "rush hours peaks".

Table 1: Coefficients of eqs. (3) and (6) for working (w) and non-working (nw) days (velocities in mm/sec and densities in ped/m^2).

	v_{ρ_0} (w)	b_ρ (w)	v_0 (w)	b_r (w)	v_{ρ_0} (nw)	b_ρ (nw)	v_0 (nw)	b_r (nw)
all pedestrians	1210	-898			1142	-1479		
tall	1239	-692	1314	-313	1165	-1557	1118	-186
short	1148	-1286			1111	-1367		

4.5. Dependence of velocity of "tall people" on the number of "short" ones

Fig. 7b shows all the 20 minute slots data points for the "tall people" velocity versus the ratio

$$r = \frac{\rho_{short}}{\rho} \tag{5}$$

of the "short people" density over overall density (number of short people over overall pedestrians), compared to a linear model

$$v(r) = v_0 + b_r r. \tag{6}$$

Even though the variation around the linear fit is large, the linear model for the working days seems to describe well the dependence of velocity on such a parameter (on non-working days the variation of the ratio of short people is more reduced). We may try to use a double linear model to correct the adult velocities accounting for the density and ratio of "short" people ("normalised tall people velocity") as

$$v_0(t) = v(t) - b_\rho \rho - b_r (r - 0.5). \tag{7}$$

Interestingly, as shown in Fig. 8c, after such an operation the working and non-working day distribution look quite similar[17]. Obviously, the peculiar behaviour at the rush hours is still present.

[17] Nevertheless, the linear models are different for working days and non-working days, so the quantitative similarity would change if, for example, we decided to show the data for a value of the ratio different from 0.5.

5. Conclusions

Using an automatic tracking system, we collected more than 800 hours of pedestrian movement data in a real world environment. By studying the pedestrian density and velocity patterns in a corridor of this environment, we verified that Japanese pedestrians have a tendency to walk on the left side of the corridor, but that such a splitting of flows converges to zero for very low densities (at least in a narrow and slightly irregular environment as the one investigated in this paper). Furthermore, we verified that as the density and the separation of flows increase, fast pedestrians move towards the right side of the corridor.

We also studied the factors that influence the pedestrian velocity, finding that pedestrian velocity decreases, as expected, with density, but that many other variables have to be taken in consideration. Since we verified that taller people walk faster, the number of tall people influences obviously the overall pedestrian velocity. Nevertheless, the same velocity of the tall people is influenced by the presence of short people (due probably also to the presence of groups with adults and children). Most important, in different moments of the day people may show different behaviours influencing their velocity (rush hours), and a general tendency of walking slowly in late hours is present (tiredness?). Our findings suggest that many factors have to be taken in account when studying the variation in velocity in a crowd, even when the environment is kept fixed.

References

Bauer, D., Brandle, N., Seer, S., Ray, M., Kitazawa, K., 2009. Measurement of pedestrian movements: A comparative study on various existing systems, in: Pedestrian Behavior: Models, Data Collection and Applications. Emerald, pp. 325–344.

Brščić, D., Kanda, T., Ikeda, T., Miyashita, T., 2013. Person tracking in large public spaces using 3-d range sensors. IEEE Transactions on Human Machine Systems 43, 522–534.

Burstedde, C., Klauck, K., Schadschneider, A., Zittartz, J., 2001. Simulation of pedestrian dynamics using a two-dimensional cellular automaton. Physica A: Statistical Mechanics and its Applications 295, 507–525.

Guy, S., Curtis, S., Lin, M., Manocha, D., 2012. Least-effort trajectories lead to emergent crowd behaviors. Physical Review E 85, 016110.

Helbing, D., Farkas, I., Molnar, P., Vicsek, T., 2002. Simulation of pedestrian crowds in normal and evacuation situations, in: Pedestrian and Evacuation Dynamics. Springer, pp. 21–58.

Helbing, D., Molnar, P., 1995. Social force model for pedestrian dynamics. Phys. Rev. E 51, 4282–4286.

Kachroo, P.P., Al-Nasur, S.J., Wadoo, S.A., 2008. Pedestrian dynamics: Feedback control of crowd evacuation. Springer.

Moussaïd, M., Helbing, D., Garnier, S., Johansson, A., Combe, M., Theraulaz, G., 2009. Experimental study of the behavioural mechanisms underlying self-organization in human crowds. Proceedings of the Royal Society B: Biological Sciences 276, 2755–2762.

Muramatsu, M., Nagatani, T., 2000. Jamming transition of pedestrian traffic at a crossing with open boundaries. Physica A: Statistical Mechanics and its Applications 286, 377–390.

Seyfried, A., Steffen, B., Klingsch, W., Boltes, M., 2005. The fundamental diagram of pedestrian movement revisited. Journal of Statistical Mechanics: Theory and Experiment 2005, P10002.

Zanlungo, F., 2007. A collision avoiding mechanism based on a theory of mind. Advances in complex systems 10, 363–371.

Zanlungo, F., Chigodo, Y., Ikeda, T., Kanda, T., 2014. Experimental study and modelling of pedestrian space occupation and motion pattern in a real world environment, in: Pedestrian and Evacuation Dynamics 2012. Springer. volume I, pp. 289–304.

Zanlungo, F., Ikeda, T., Kanda, T., 2011. Social force model with explicit collision prediction. EPL (Europhysics Letters) 93, 68005.

Zanlungo, F., Ikeda, T., Kanda, T., 2012. A microscopic social norm model to obtain realistic macroscopic velocity and density pedestrian distributions. PloS one 7, e50720.

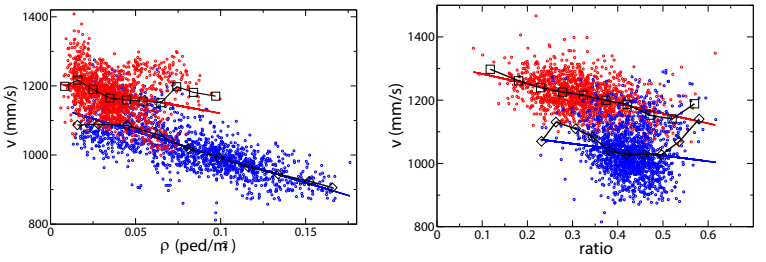

(a) (b)

Fig. 7: (a): velocity (best fitting Gaussian centre) versus density distribution on working days (red) and non-working days (blue), compared to linear best fits (eq. 3) in the same colour and to average values over an appropriate density range (black-squares for working days, black-diamonds for non-working days). (b): velocity versus short/overall ratio in working days non-working days, compared to linear best fits (eq. 6) and to average values over an appropriate density range, same colours as (a).

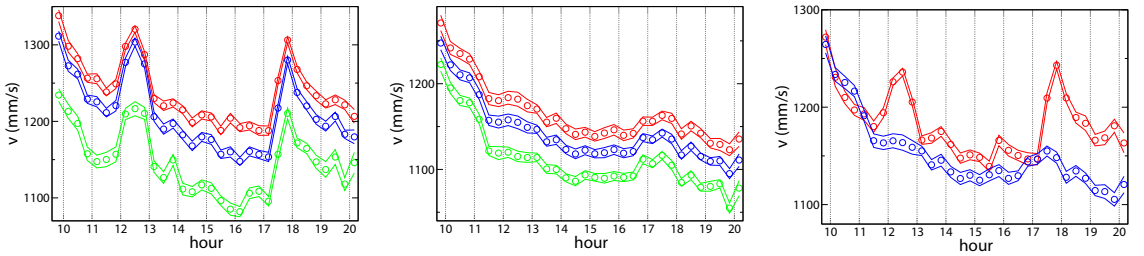

(a) (b) (c)

Fig. 8: (a) :"zero density velocity" v_{ρ_0} (extrapolated from the data of Fig. 6 using in eq. (4) the linear model of Fig. 7a and Table 1) as a function of the hour of a working day; all pedestrians in blue, "tall people" in red, "short people" in green. (b): same graph for non-working days. (c): "normalised tall people velocity" v_0 (extrapolated from the "tall people" data of Fig. 6 using in eq. (7) the linear models of figures 7 and Table 1) as a function of the hour of the day.